Eur. J. Mineral.
2016, **28**, 687–696
Published online 1 April 2016

Castellaroite, $Mn^{2+}_3(AsO_4)_2 \cdot 4.5H_2O$, a new mineral from Italy related to metaswitzerite

ANTHONY R. KAMPF[1,*], FERNANDO CÁMARA[2,3], MARCO E. CIRIOTTI[4], BARBARA P. NASH[5], CORRADO BALESTRA[6] and LUIGI CHIAPPINO[7]

[1] Mineral Sciences Department, Natural History Museum of Los Angeles County, 900 Exposition Boulevard, Los Angeles, CA 90007, USA
[*]Corresponding author, e-mail: akampf@nhm.org
[2] Dipartimento di Scienze della Terra, Università degli Studi di Torino, Via Tommaso Valperga Caluso 35, 10125 Torino, Italy
[3] CrisDi, Interdepartmental Centre for the Research and Development of Crystallography, via Pietro Giuria 5, 10125, Torino, Italy
[4] Associazione Micromineralogica Italiana, via San Pietro 55, 10073 Devesi-Cirié, Torino, Italy
[5] Department of Geology and Geophysics, University of Utah, Salt Lake City, Utah 84112, USA
[6] Associazione Micromineralogica Italiana, via Luigi Delfino 74, 17017 Millesimo, Savona, Italy
[7] via Palmanova 67, 20132 Milano, Italy

Abstract: Castellaroite (IMA2015-071), $Mn^{2+}_3(AsO_4)_2 \cdot 4.5H_2O$, is a new secondary arsenate mineral from the Monte Nero mine, Rocchetta Vara, La Spezia, Liguria, Italy and the Valletta mine, near Canosio, Cuneo, Piedmont, Italy. It crystallized from As- and Mn-rich hydrothermal fluids in an oxidizing environment. At Monte Nero, it is associated with coralloite, manganohörnesite, rhodochrosite, sarkinite, sterlinghillite, strashimirite and wallkilldellite. At Valletta, it is associated with braccoite, hematite, manganberzeliite, orthoclase and tiragalloite. Castellaroite occurs as thin blades, flattened on [001], striated and elongated parallel to [100] and exhibiting the forms {110}, {012} and {001}. The mineral is colourless and transparent with a vitreous to silky lustre and white streak. Crystals are flexible with a curved fracture, and one perfect cleavage on {001}. The Mohs' hardness is 2½. The measured and calculated densities are 3.14(2) g·cm^{-3} and 3.164 g·cm^{-3}, respectively. The mineral is easily soluble in dilute HCl at room temperature. Optically, castellaroite crystals are biaxial (–), with α = 1.644(1), β = 1.662(1) and γ = 1.667(1) (white light); $2V$ = 57(1)°; dispersion $r < v$, moderate; the optical orientation Y = **b**; $Z \approx$ **a**. The Raman spectrum is dominated by features corresponding to the AsO_4 group and also confirms the presence of H_2O. Electron-microprobe analyses gave the empirical formula $Mn^{2+}_{3.02}(As_{1.94}P_{0.06})_{\Sigma 2.00}O_{12.5}H_{8.96}$, based on 12.5 O *apfu*. Castellaroite is monoclinic, $P2_1/n$, with the unit-cell parameters: a = 8.7565(8), b = 13.4683(13), c = 18.652(2) Å, β = 94.876(7)°, V = 2191.7(4) Å^3 and Z = 8. The eight strongest lines in the X-ray powder diffraction pattern are [d_{obs}/Å (I) (hkl)]: 10.90(100)(011), 9.27(67)(002), 6.97(42)($\bar{1}$11), 3.323(47)(multiple), 3.043(87)($\bar{1}$34,204,$\bar{2}$32), 2.656(85)(multiple), 2.165(46)(multiple), and 1.5589(32)(multiple). The crystal structure was refined to R_1 = 0.118 for 2513 observed reflections [$F_o > 4\sigma F$]. The structure contains kinked chains of edge-sharing MnO_6 octahedra parallel to [100]. The chains are linked to each other by corner-sharing, forming sheets parallel to {001} and AsO_4 tetrahedra corner-link with octahedra in the sheet, forming a heteropolyhedral layer. Edge-sharing MnO_6–MnO_5 dimers share corners with octahedra and tetrahedra in adjacent layers, thereby linking them in the [001] direction. The heteropolyhedral layer is topologically identical to those in the structures of the phosphate minerals: angarfite, bakhchisaraitsevite, mejillonesite, metaswitzerite, rimkorolgite and switzerite. Overall, the structure is most similar to that of metaswitzerite.

Key-words: castellaroite; arsenate; crystal structure; Raman spectroscopy; Monte Nero mine; Valletta mine; Italy.

1. Introduction

Long inactive manganese deposits, also rich in arsenic, in the Alpine tectono-metamorphic terrains of north-western Italy have yielded a variety of interesting secondary hydrothermal minerals. Among these deposits, the Molinello and Gambatesa mines in Val Graveglia, Liguria, are well known (*cf.* Marchesini & Pagano, 2001), having yielded eight and six new mineral species, respectively. Two lesser-known mines, the Monte Nero mine in Liguria and the Valletta mine in Piedmont have also yielded new species: coralloite (Callegari *et al.*, 2012) from Monte Nero and braccoite (Cámara *et al.*, 2015), canosioite (Cámara *et al.*, 2016) and grandaite (Cámara *et al.*, 2014) from Valletta. Herein, we describe the new mineral castellaroite from both the Monte Nero mine and the Valletta mine.

0935-1221/16/0028-2535 $ 4.50
DOI: 10.1127/ejm/2016/0028-2535

The name castellaroite honours Fabrizio Castellaro (born 1970) of Mezzanego, Italy. Mr. Castellaro is an avid and sophisticated mineral collector specializing in the minerals of Liguria. He is the discoverer of castellaroite and has also discovered the new minerals balestraite, cerchiaraite-(Fe) and 1*M* O-D polytype of lavinskyite ("liguriaite"; IMA2014-035). Mr. Castellaro has agreed to the naming of the mineral in his honour.

The mineral and name (IMA2015–071) were approved by the IMA–CNMNC prior to publication. The description is based upon one holotype and three cotype specimens. The holotype and one cotype, both from the Monte Nero mine, are deposited in the collections of the Natural History Museum of Los Angeles County, 900 Exposition Boulevard, Los Angeles, CA 90007, USA, catalogue numbers 65603 (holotype) and 65604 (cotype). Two cotypes are deposited in the mineralogical collections of the Dipartimento di Scienze della Terra of the Università di Torino stored in the Museo Regionale di Scienze Naturali di Torino, Sezione di Mineralogia, Petrografia e Geologia, via Giovanni Giolitti 36, I-10123 Torino, Italy, catalogue numbers M/U 16950 (Monte Nero) and M/U 16951 (Valletta).

2. Occurrence

The new mineral was discovered by Fabrizio Castellaro on two specimens collected from the "classic" dump at the Monte Nero mine, Rocchetta Vara, La Spezia, Liguria, Italy (44°14'48''N, 9°45'27''E). The deposit is comprised of thin manganese stratiform ores that are located near the base of a chert sequence in the "Diaspri di Monte Alpe" formation, which overlies Jurassic ophiolites of the Bracco unit. Castellaroite is a secondary mineral that crystallized from As- and Mn-rich fluids, which circulated through a system of fractures during the final tectono-metamorphic stage of the deposit (Marescotti & Cabella, 1996). Other secondary minerals found with castellaroite include coralloite, manganohörnesite, rhodochrosite, sarkinite, sterlinghillite, strashimirite and wallkilldellite. The Monte Nero mine is also the type locality for coralloite (Callegari *et al.*, 2012). More information on the deposit can be found in Callegari *et al.* (2012) and references therein.

Castellaroite has also been found on specimens recovered from the dumps of the Valletta mine, near Canosio, Piedmont, Italy (44°23'42''N, 7°5'42''E), where it was identified by SEM-EDX and Raman spectroscopy, and this is considered to be a cotype locality. The Valletta mine is a small Fe-Mn deposit that has not been worked in modern times and has never been studied geologically or petrologically. The geological setting is rather similar to that of the Monte Nero mine and has been summarized by Cámara *et al.* (2014) in their description of the new mineral grandaite, for which the Valletta mine is also the type locality. At the Valletta mine, castellaroite is a secondary mineral crystallized from hydrothermal fluids in an oxidizing environment. It is associated with braccoite, hematite, manganberzeliite, orthoclase and tiragalloite.

3. Physical and optical properties

At the Monte Nero mine, castellaroite occurs in radial aggregates up to about 5 mm in diameter consisting of very thin blades, and rarely as individual crystals up to about 2 mm in length (Fig. 1). At the Valletta mine, it forms aggregates of thin blades up to about 0.5 mm in length. Blades are flattened on [001], striated and elongated parallel to [100] and exhibit the forms {110}, {012} and {001} (Fig. 2). No twinning was observed. Crystals are colourless and transparent with a vitreous to silky lustre and white streak. The mineral is non-fluorescent. Crystals are flexible with a curved fracture, and one perfect cleavage on {001}. The Mohs' hardness is 2½, based upon scratch tests. The density measured by floatation in Clerici solution is 3.14(2) $g \cdot cm^{-3}$. The calculated density is 3.164 $g \cdot cm^{-3}$, based on the empirical formula, and 3.174 $g \cdot cm^{-3}$, based on the ideal formula. The mineral is easily soluble in dilute HCl at room temperature. Optically, castellaroite crystals are biaxial (–), with $\alpha = 1.644(1)$, $\beta = 1.662(1)$ and $\gamma = 1.667(1)$, measured in white light. The $2V$ measured directly on a spindle stage is 57(1)°; the calculated $2V$ is 55°. Dispersion is $r < v$, moderate and the optical orientation is $Y = \mathbf{b}$; $Z \approx \mathbf{a}$. The mineral is nonpleochroic. The Gladstone–Dale compatibility (Mandarino, 2007) is –0.019, in the range of superior compatibility, based upon the empirical formula.

4. Raman spectroscopy

The Raman spectra of castellaroite (Figs 3 and 4) from both the Monte Nero mine and the Valletta mine were obtained at the Dipartimento di Scienze della Terra (Università di Torino) using a micro/macro Jobin Yvon Mod. LabRam HRVIS, equipped with a motorized x-y stage and an Olympus microscope. The backscattered Raman signal was collected with 50× objective and the

Fig. 1. Castellaroite crystals from the Monte Nero mine. Field of view is 4 mm across.

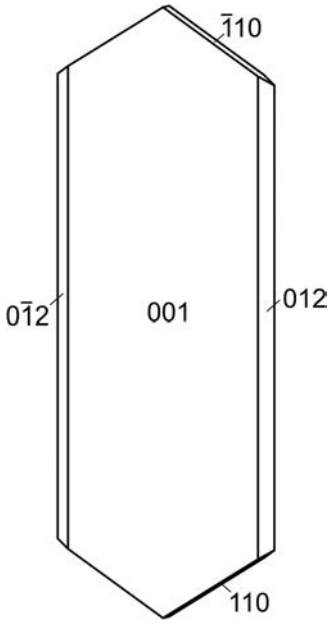

Fig. 2. Crystal drawing of castellaroite, clinographic projection in nonstandard orientation, [100] vertical.

Raman spectra were obtained for non-oriented crystals. The 532 nm line of a solid-state Nd laser was used for excitation; laser power (250 mW) was controlled by means of a series of density filters. The minimum lateral and depth resolution was set to a few μm. The system was calibrated using the 520.6 cm^{-1} Raman band of silicon before each experimental session. The spectra were collected with multiple acquisitions (2–3) with single counting times ranging between 20 and 30 s. The spectra were recorded using the LabSpec 5 program from 100 to 4000 cm^{-1}. Note that the spectrum obtained for the sample from Valletta is much weaker and, therefore, less well resolved; we only report it here from 100 to 1100 cm^{-1}. Band component analysis was undertaken using the Fityk software package (Wojdyr, 2010).

The Raman spectra confirmed the presence of $(AsO_4)^{3-}$. The most characteristic features of the castellaroite spectra are observed in the region of 600–950 cm^{-1} (values observed for Valletta material are reported in italics), where the spectra consist of four main overlapping bands observed at 800.5(*800.4*), 822.2(*821.9*), 846.8 (*843.5*) and 862.5(*869.9*) cm^{-1}, with two weaker shoulders at 910.6(*910.2*) and 933.8 cm^{-1}, the latter not well resolved in the Valletta spectrum (Fig. 3) because it is much weaker. The most intense bands of that group are the one at 862.5 cm^{-1}, which can be interpreted as the ν_1 AsO_4 symmetric stretching vibration, and the one at 800.5 cm^{-1}, which can be interpreted as the ν_3 AsO_4 antisymmetric stretching vibration. The band at 846.8 (*843.5*) is not well resolved for the Monte Nero sample and only weakly for the Valletta sample. The weak bands at 910.6(*910.2*) and 933.8 cm^{-1} could be interpreted as water vibrational modes (Martens *et al*., 2004). At wavenumbers 300–600 cm^{-1}, a prominent band centred at 425.6(*426.5*) cm^{-1} is flanked on one side by two well-resolved peaks at 340(*346.9*) and 371.5(*376.1*) and on the other by a peak at 459.4(*447.2*) cm^{-1}. The bands at 425.6 and 459.4 cm^{-1} can be interpreted as the ν_2 AsO_4 symmetric bending modes, and the ones at 340 and 371.5 cm^{-1} as the ν_4 AsO_4 antisymmetric bending modes. Two weaker bands observed at 503.6 and 577.5 cm^{-1} are difficult to assign and may be related to the stretching of MnO_6 groups. In the lattice vibrations

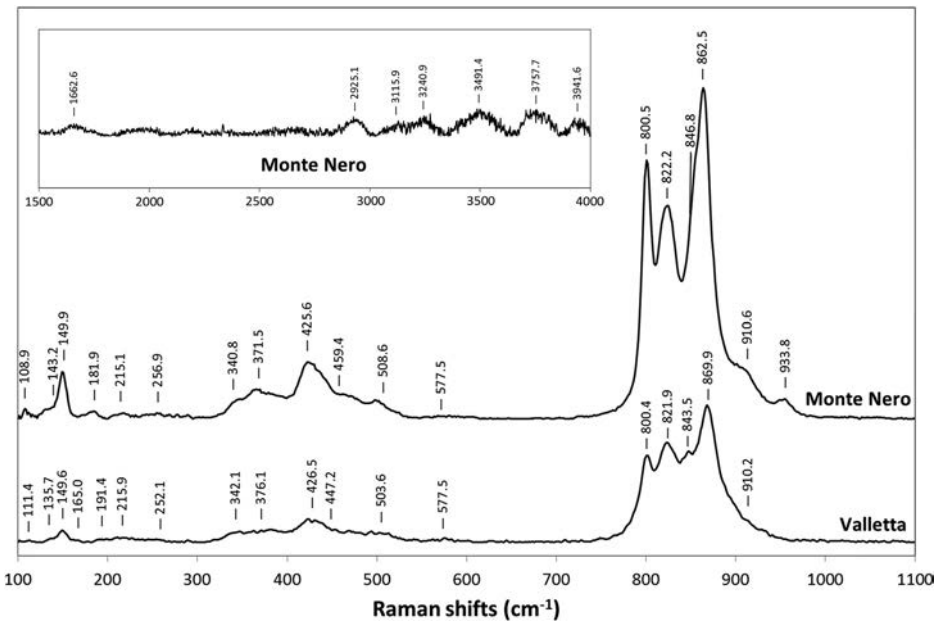

Fig. 3. Raman spectra of castellaroite from the Monte Nero and Valletta mines in the 100–1100 cm^{-1} range and, in the insert, the Raman spectrum of castellaroite from Monte Nero in the 1500–4000 cm^{-1} range.

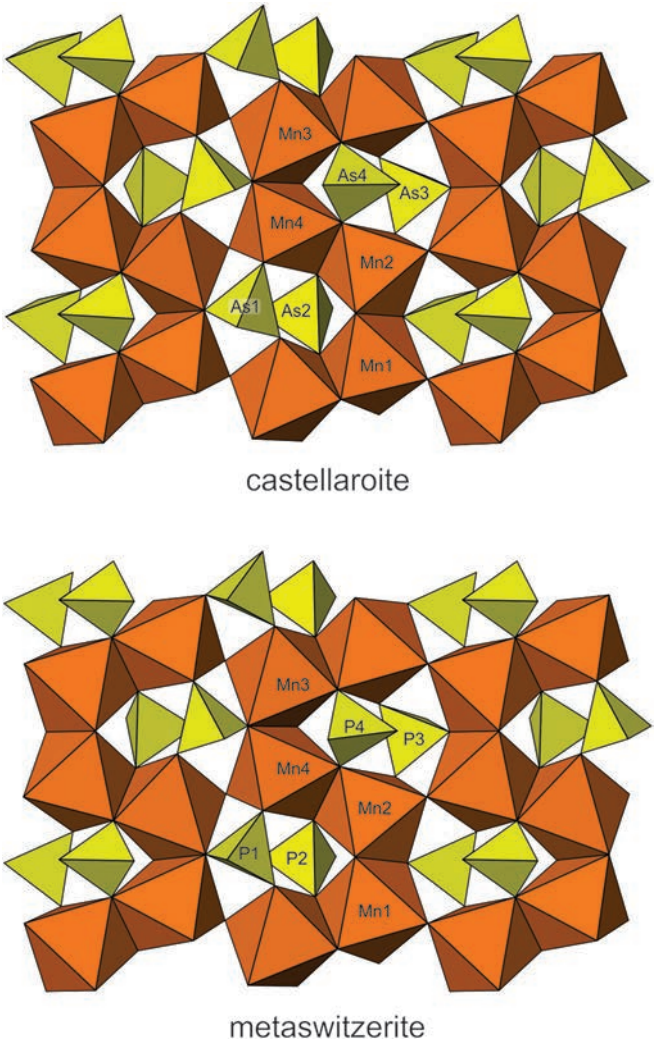

Fig. 4. Polyhedral layers parallel to {001} in castellaroite and metaswitzerite, viewed with [100] vertical. (online version in colour)

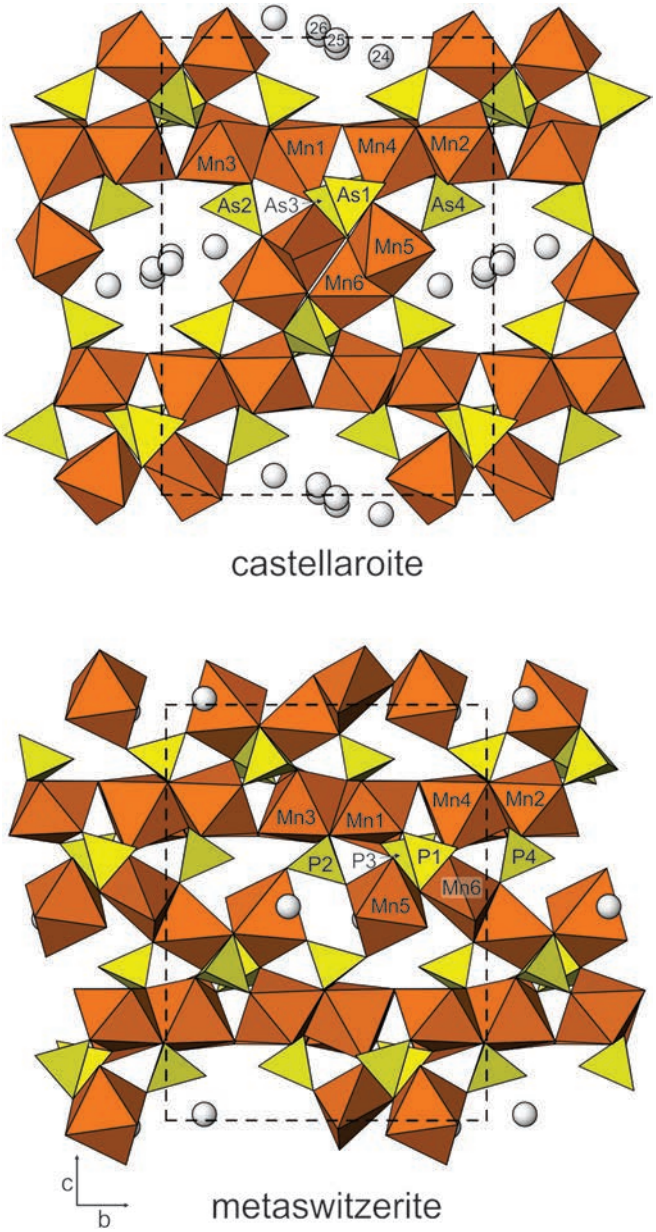

Fig. 5. The crystal structures of castellaroite and metaswitzerite viewed parallel to {100}. The channel H_2O groups are shown as white spheres and are numbered for the castellaroite structure. The unit cells are shown by dashed lines. (online version in colour)

range (< 300 cm^{-1}), five weakly resolved bands can be recognized for the Monte Nero sample at 108.9, 149.9, 181.9, 215.1 and 256.9 cm^{-1}, with a shoulder at 143.2 cm^{-1}. The same bands are observed for the Valletta sample at *111.4, 149.6, 177.8, 215.9* and *252.1* cm^{-1}, with the shoulder shifted to lower wavenumbers and better resolved (*135.7* cm^{-1}) and a band at *177.8* that is very weak and split into two shoulders of adjacent bands at lower and higher wavenumbers (*165.0, 191.4*) (Fig. 3).

Regarding H_2O group bending and stretching vibrations, in the spectrum for the Monte Nero sample, a very weak band centred at 1662.6 cm^{-1} is observed, which could be interpreted as the bending vibrations of the H_2O. The bands due to hydroxyl stretching modes of the H_2O groups are observed at 2925.1, 3115.9, 3240.9, 3491.4, 3757.7 and 3941.6 cm^{-1}, reflecting the complex nature of the hydrogen bonding on castellaroite (Fig. 3). Note that because of the paucity of material IR spectroscopy was not attempted.

Table 1. Analytical data (in wt%) for castellaroite.

Constituent	Mean	Range	SD	Standard
MnO	41.62	40.33–42.82	0.63	rhodonite
As_2O_5	43.35	41.83–44.64	0.75	syn. GaAs
P_2O_5	0.82	0.61–1.23	0.16	apatite
H_2O*	15.69			
Total	101.48			

* Calculated on the basis of As + P = 2 *apfu*, charge balance and O = 12.5 *apfu*.

5. Chemical composition

Quantitative analyses (28 points on 7 crystals from Monte Nero) were performed at the University of Utah on a Cameca SX-50 electron microprobe with four wavelength-dispersive spectrometers (WDS). Analytical conditions were: 15 kV accelerating voltage, 20 nA beam current and a beam diameter of 10–15 μm. Castellaroite exhibited minor damage under the electron beam. Counting times were 20 s on peak and 10 s on + and – background. No other elements than O, P, Mn and As were detected by energy-dispersive spectrometry. Other likely elements were sought by WDS,

Table 2. Powder X-ray data (d in Å) for castellaroite. Only calculated lines with $I > 1$ are shown.

I_{obs}	d_{obs}	d_{calc}	I_{calc}	hkl	I_{obs}	d_{obs}	d_{calc}	I_{calc}	hkl
100	10.90	10.9056	100	0 1 1			2.1812	4	4 0 0
67	9.27	9.2922	84	0 0 2	46	2.165	2.1726	6	3 1 5
		7.6485	4	0 1 2			2.1648	10	$\bar{4}$ 0 2
42	6.97	6.9849	28	$\bar{1}$ 1 1			2.1539	6	1 6 1
26	6.63	6.6529	22	1 1 1	7	2.088	2.0925	2	3 2 5
		5.6280	3	0 1 3			2.0848	2	0 4 7
		5.5618	5	1 1 2			2.0632	2	0 3 8
11	5.20	5.1963	7	$\bar{1}$ 2 1			2.0424	2	$\bar{4}$ 0 4
		4.7313	5	$\bar{1}$ 2 2	10	2.0355	2.0378	2	1 6 3
9	4.609	4.5714	10	1 1 3			2.0261	3	$\bar{3}$ 1 7
10	4.373	4.3624	7	2 0 0	7	1.9505	1.9660	2	2 3 7
		4.1487	3	$\bar{1}$ 2 3			1.9357	2	4 3 1
12	4.031	4.0424	8	0 3 2	6	1.9218	1.9129	2	4 0 4
		3.9920	2	1 3 0	9	1.8951	1.8906	3	4 3 2
		3.8721	2	1 3 1			1.8646	2	3 1 7
11	3.830	3.8258	6	2 0 2	18	1.8590	1.8593	2	$\bar{4}$ 0 6
17	3.692	3.7207	8	$\bar{1}$ 3 2			1.8585	6	0 0 10
		3.6352	11	0 3 3			1.8576	3	$\bar{3}$ 5 4
		3.6172	3	1 3 2			1.7877	2	$\bar{2}$ 6 5
24	3.594	3.5963	22	$\bar{1}$ 2 4	6	1.7504	1.7603	4	0 4 9
9	3.453	3.4158	18	1 2 4			1.7464	3	$\bar{1}$ 5 8
47	3.323	3.3244	22	$\bar{2}$ 0 4	9	1.7167	1.7225	3	4 4 3
		3.3131	3	0 4 1			1.6988	2	$\bar{3}$ 2 9
		3.2285	6	0 3 4			1.6885	2	3 2 8
		3.2229	2	1 1 5	13	1.6830	1.6851	5	3 6 3
20	3.115	3.1286	7	2 3 0			1.6764	2	0 1 11
		3.1261	12	$\bar{1}$ 2 5			1.6384	2	5 2 2
		3.0878	3	$\bar{1}$ 3 4	18	1.6295	1.6366	7	$\bar{3}$ 6 5
87	3.043	3.0534	50	2 0 4			1.6312	2	$\bar{5}$ 2 4
		3.0213	15	$\bar{2}$ 3 2			1.6240	4	3 5 6
17	2.961	2.9773	6	1 2 5			1.5967	2	5 2 3
		2.9583	5	0 4 3			1.5928	3	2 4 9
		2.9119	9	2 3 2	20	1.5819	1.5844	4	$\bar{3}$ 2 10
18	2.894	2.8872	3	$\bar{2}$ 1 5			1.5828	3	0 8 4
		2.8638	8	$\bar{2}$ 3 3			1.5750	2	3 2 9
		2.7407	6	$\bar{1}$ 2 6			1.5717	4	3 6 5
		2.7264	4	0 4 4			1.5706	2	2 8 0
		2.6723	8	$\bar{3}$ 2 1			1.5691	3	$\bar{2}$ 8 1
		2.6699	12	3 2 0	32	1.5589	1.5600	2	$\bar{4}$ 4 7
85	2.656	2.6638	5	2 1 5			1.5588	2	$\bar{4}$ 3 8
		2.6579	18	$\bar{2}$ 4 1			1.5565	4	$\bar{2}$ 8 2
		2.6334	18	$\bar{2}$ 0 6			1.5472	3	5 2 4
17	2.614	2.6197	7	1 2 6			1.5371	4	$\bar{5}$ 2 6
8	2.566	2.5872	6	0 5 2	15	1.5290	1.5336	3	0 8 5
		2.5495	8	0 3 6			1.5133	4	$\bar{1}$ 6 9
15	2.492	2.4954	13	0 4 5	6	1.4760	1.4816	3	1 6 9
		2.4646	3	1 5 2			1.4617	2	$\bar{2}$ 4 11
3	2.418	2.4033	4	$\bar{3}$ 3 2	19	1.4550	1.4557	2	$\bar{6}$ 0 2
4	2.327	2.3303	4	0 5 4			1.4395	2	$\bar{1}$ 9 3
		2.3231	2	0 0 8	10	1.4296	1.4229	2	$\bar{2}$ 3 12
		2.2852	2	0 3 7	12	1.3783	1.3807	4	$\bar{5}$ 6 1
7	2.216	2.2285	2	0 6 1					
		2.2214	3	$\bar{2}$ 4 5					

but none were above the detection limits. Raw X-ray intensities were corrected for matrix effects with a $\phi(\rho z)$ algorithm (Pouchou & Pichoir, 1991). Because insufficient material was available for a direct determination of H_2O, the amount of water was calculated on the basis of As + P = 2 atoms per formula unit (*apfu*), charge balance and O = 12.5 *apfu*, as determined by the crystal-structure analysis which also confirmed the divalent state of Mn (see below). Analytical data are given in Table 1. The empirical formula is $Mn^{2+}_{3.02}(As_{1.94}P_{0.06})_{\Sigma 2.00}O_{12.5}H_{8.96}$. The simplified structural formula is $Mn^{2+}(AsO_4)_2 \cdot 4.5H_2O$, which requires MnO 40.63, As_2O_5 43.89, H_2O 15.48, total 100 wt%.

6. X-ray crystallography and crystal-structure determination

Powder X-ray diffraction data for castellaroite were obtained on a Rigaku R-Axis Rapid II curved–imaging-plate microdiffractometer utilising monochromatised Mo*K*α radiation. A Gandolfi-like motion on the φ and ω axes was used to randomize the sample. Observed *d* spacings and intensities were derived by profile fitting using JADE 2010 software (Materials Data Inc.). Data are given in Table 2. The unit-cell parameters refined from the powder data using JADE 2010 with whole-pattern fitting are: $a = 8.733(4)$, $b = 13.438(4)$, $c = 18.643(4)$ Å, $\beta = 95.006(11)°$ and $V = 2179.5(13)$ Å^3.

Single-crystal structure data were obtained on the same instrument noted above. The Rigaku CrystalClear software package was used for processing of structure data, including the application of an empirical multi-scan absorption correction using ABSCOR (Higashi, 2001). The structure was solved by direct methods using SIR2011 (Burla *et al.*, 2012). SHELXL-97 (Sheldrick, 2008) was used for the refinement of the structure, with scattering curves for neutral atoms (Wilson, 1992). The As and Mn sites were refined with fixed full occupancy. Two O sites in the channel of the structure refined to approximately ½ occupancy and were assigned exactly ½ occupancy in the final refinement. The poor diffraction quality of crystals caused by a strong tendency toward crystal warping resulted in the high *R* factors and large electron-density residuals. In spite of the poor diffraction quality, it was possible to refine anisotropic displacement parameters for all atoms. The very reasonable bond lengths, polyhedral geometries and bond-valence sums corroborate the correctness of the structure. Data collection and refinement details are given in Table 3, atom coordinates and displacement parameters in Table 4, selected bond distances in Table 5 and a bond valence analysis in Table 6. The Crystallography Information File (CIF), including reflection data, is available online as supplementary material linked to this article on the GSW website of the journal, http://eurjmin.geoscienceworld.org.

Table 3. Data collection and structure refinement details for castellaroite.

Diffractometer	Rigaku R-Axis Rapid II
X-ray radiation/power	Mo*K*α ($\lambda = 0.71075$ Å)/50 kV, 40 mA
Temperature	293(2) K
Structural formula	$Mn_3(AsO_4)_2 \cdot 4.5H_2O$
Space group	$P2_1/n$
Unit-cell dimensions	$a = 8.7565(8)$ Å
	$b = 13.4683(13)$ Å
	$c = 18.652(2)$ Å
	$\beta = 94.876(7)°$
V	2191.7(4) Å^3
Z	8
Density (for above formula)	3.174 g·cm^{-3}
Absorption coefficient	9.458 mm^{-1}
F(000)	2000
Crystal size	240 × 45 × 5 μm
θ range	3.03–25.25°
Index ranges	$-10 \le h \le 10$, $-15 \le k \le 15$, $-22 \le l \le 22$
Refls. collected/unique	17418/3407; $R_{int} = 0.093$
Reflections with $F > 4\sigma(F)$	2513
Completeness to θ = 19.96°	85.9 %
Max. and min. transmission	0.954 and 0.210
Refinement method	Full-matrix least-squares on F^2
Parameters/restraints	325/0
GoF	1.346
Final *R* indices [$F_o > 4\sigma(F)$]	$R_1 = 0.1182$, $wR_2 = 0.3270$
R indices (all data)	$R_1 = 0.1365$, $wR_2 = 0.3503$
Largest diff. peak/hole	+4.87/–3.68 *e*/Å^3

*$R_{int} = \Sigma|F_o^2 - F_o^2(\text{mean})|/\Sigma[F_o^2]$. GoF = $S = \{\Sigma[w(F_o^2 - F_c^2)^2]/(n-p)\}^{1/2}$. $R_1 = \Sigma||F_o| - |F_c||/\Sigma|F_o|$. $wR_2 = \{\Sigma[w(F_o^2 - F_c^2)^2]/\Sigma[w(F_o^2)^2]\}^{1/2}$; $w = 1/[\sigma^2(F_o^2) + (aP)^2 + bP]$ where *a* is 0.2, *b* is 0 and *P* is $[2F_c^2 + \text{Max}(F_o^2, 0)]/3$.

Table 4. Atom fractional coordinates and displacement parameters (Å^2) for castellaroite.

	x	*y*	*z*	U_{eq}	U^{11}	U^{22}	U^{33}	U^{23}	U^{13}	U^{12}
Mn1	0.9614(3)	0.58628(18)	0.26437(14)	0.0238(7)	0.0210(15)	0.0110(14)	0.0400(17)	0.0017(9)	0.0063(10)	-0.0004(10)
Mn2	0.5628(3)	0.58800(18)	0.26092(14)	0.0233(7)	0.0200(14)	0.0149(15)	0.0349(16)	0.0021(9)	0.0018(10)	-0.0001(10)
Mn3	0.4562(3)	0.31797(18)	0.25484(14)	0.0235(7)	0.0208(14)	0.0109(15)	0.0395(17)	-0.0016(9)	0.0061(10)	-0.0001(10)
Mn4	0.0640(3)	0.31829(17)	0.25889(14)	0.0232(7)	0.0177(14)	0.0118(15)	0.0401(17)	-0.0010(9)	0.0027(10)	-0.0029(10)
Mn5	0.1037(3)	0.31049(19)	0.45711(15)	0.0275(7)	0.0219(15)	0.0221(16)	0.0384(17)	-0.0039(10)	0.0021(11)	-0.0003(10)
Mn6	0.3812(3)	0.42197(18)	0.54981(14)	0.0267(7)	0.0263(15)	0.0162(15)	0.0373(17)	0.0000(10)	0.0009(10)	-0.0040(10)
As1	0.21688(18)	0.58951(13)	0.64641(9)	0.0228(6)	0.0208(11)	0.0128(11)	0.0353(12)	0.0004(6)	0.0048(7)	-0.0006(6)
As2	0.23328(19)	0.23738(13)	0.64198(9)	0.0244(6)	0.0211(11)	0.0162(11)	0.0363(12)	0.0015(6)	0.0046(7)	-0.0005(7)
As3	0.28564(18)	0.48655(12)	0.36085(9)	0.0215(6)	0.0183(10)	0.0115(11)	0.0350(12)	-0.0011(6)	0.0033(7)	-0.0014(6)
As4	0.27166(18)	0.14694(14)	0.35133(9)	0.0245(6)	0.0208(11)	0.0158(11)	0.0372(12)	-0.0007(6)	0.0052(7)	0.0007(7)
O1	0.6658(13)	0.3246(8)	0.3185(7)	0.031(3)	0.026(6)	0.016(6)	0.050(8)	-0.002(5)	-0.008(5)	-0.006(5)
O2	0.2718(12)	0.5586(8)	0.5659(6)	0.032(3)	0.020(6)	0.021(7)	0.056(9)	-0.001(5)	0.014(5)	0.012(5)
O3	0.7709(12)	0.5142(8)	0.3035(6)	0.026(3)	0.019(6)	0.008(6)	0.051(8)	0.007(4)	0.003(5)	0.005(5)
O4	0.9644(11)	0.3663(8)	0.3585(6)	0.023(2)	0.020(6)	0.016(6)	0.033(7)	-0.007(4)	0.000(4)	0.002(4)
O5	0.2281(12)	0.1159(9)	0.6288(6)	0.029(3)	0.024(6)	0.028(7)	0.036(7)	-0.006(5)	0.006(5)	0.006(5)
O6	0.5765(12)	0.2280(8)	0.1810(6)	0.026(3)	0.020(6)	0.014(6)	0.045(8)	-0.006(4)	0.012(5)	-0.002(5)
O7	0.2409(13)	0.3026(8)	0.5653(6)	0.029(3)	0.033(7)	0.026(7)	0.027(7)	-0.009(5)	0.001(5)	0.001(5)
O8	0.8912(11)	0.2335(8)	0.1962(6)	0.025(3)	0.009(5)	0.018(6)	0.048(8)	-0.009(5)	0.007(4)	-0.004(4)
O9	0.1599(13)	0.5728(8)	0.3372(6)	0.028(3)	0.030(7)	0.011(6)	0.043(8)	-0.004(5)	-0.004(5)	-0.003(5)
O10	0.2727(13)	0.3943(8)	0.3008(6)	0.030(3)	0.029(7)	0.029(7)	0.033(7)	0.001(5)	0.004(5)	-0.005(5)
O11	0.2603(12)	0.4389(9)	0.4422(6)	0.027(3)	0.025(6)	0.039(8)	0.020(6)	0.000(5)	0.010(4)	-0.006(5)
O12	0.4622(12)	0.5394(8)	0.3616(6)	0.027(3)	0.031(6)	0.017(6)	0.031(7)	0.001(4)	0.000(5)	-0.005(5)
O13	0.2772(12)	0.2173(8)	0.4243(6)	0.031(3)	0.022(6)	0.027(7)	0.045(8)	-0.005(5)	0.008(5)	-0.005(5)
O14	0.2710(13)	0.0260(8)	0.3696(6)	0.027(3)	0.033(7)	0.017(6)	0.031(7)	0.003(4)	0.003(5)	0.001(5)
O15	0.4225(11)	0.1762(8)	0.3056(6)	0.024(2)	0.014(5)	0.019(7)	0.040(7)	-0.004(4)	0.009(4)	-0.005(5)
O16	0.1098(12)	0.1733(8)	0.2983(6)	0.028(3)	0.020(6)	0.029(7)	0.034(7)	-0.003(5)	-0.010(4)	-0.002(5)
OW17	0.4943(12)	0.4560(8)	0.1905(6)	0.027(3)	0.023(6)	0.015(6)	0.042(7)	-0.002(4)	0.000(5)	0.004(5)
OW18	0.2432(12)	0.2744(8)	0.1769(6)	0.026(3)	0.025(6)	0.013(6)	0.040(7)	-0.010(4)	0.000(5)	0.011(5)
OW19	0.9946(12)	0.4539(8)	0.1954(6)	0.027(3)	0.024(6)	0.003(6)	0.053(8)	0.005(4)	0.006(5)	-0.005(5)
OW20	0.7623(12)	0.1379(8)	0.3212(7)	0.032(3)	0.026(7)	0.014(7)	0.058(9)	-0.006(5)	0.013(5)	0.006(5)
OW21	0.9554(16)	0.3867(13)	0.5258(8)	0.066(5)	0.056(10)	0.100(14)	0.042(9)	-0.014(8)	0.001(7)	0.038(9)
OW22	0.9491(16)	0.1751(10)	0.4646(9)	0.058(4)	0.049(9)	0.037(9)	0.089(13)	0.006(7)	0.013(7)	-0.001(7)
OW23	0.5233(13)	0.3192(9)	0.4894(7)	0.037(3)	0.025(7)	0.024(8)	0.065(10)	-0.003(5)	0.010(6)	0.000(5)
OW24	0.1836(18)	0.3389(11)	0.0422(8)	0.064(4)	0.086(12)	0.046(10)	0.061(11)	0.012(7)	0.000(8)	-0.007(8)
OW25*	0.127(3)	0.0263(19)	0.5063(12)	0.043(6)	0.067(18)	0.038(16)	0.023(14)	0.006(10)	0.005(11)	-0.003(13)
OW26*	0.379(4)	0.028(2)	0.5217(16)	0.066(9)	0.09(2)	0.05(2)	0.06(2)	-0.008(14)	0.019(17)	-0.020(17)

* OW25 and OW26 are half occupied.

Table 5. Selected bond distances (Å) for castellaroite.

Mn1–O15	2.105(11)	Mn4–O16	2.113(11)	As1–O1	1.646(11)
Mn1–O3	2.113(11)	Mn4–O8	2.158(10)	As1–O2	1.668(11)
Mn1–O9	2.121(11)	Mn4–O10	2.181(11)	As1–O3	1.679(10)
Mn1–O6	2.202(11)	Mn4–O4	2.215(10)	As1–O4	1.690(10)
Mn1–OW19	2.232(11)	Mn4–OW19	2.233(11)	<As1–O>	1.671
Mn1–OW20	2.517(12)	Mn4–OW18	2.357(11)		
<Mn1–O>	2.215	<Mn4–O>	2.210	As2–O5	1.655(12)
				As2–O6	1.674(10)
Mn2–O16	2.131(10)	Mn5–O13	2.101(11)	As2–O7	1.684(12)
Mn2–O8	2.142(11)	Mn5–OW21	2.159(14)	As2–O8	1.689(11)
Mn2–O3	2.166(10)	Mn5–O11	2.239(11)	<As2–O>	1.676
Mn2–O12	2.238(11)	Mn5–O4	2.249(11)		
Mn2–OW17	2.261(11)	Mn5–O7	2.262(12)	As3–O9	1.635(11)
Mn2–OW20	2.354(11)	Mn5–OW22	2.282(14)	As3–O10	1.670(11)
<Mn2–O>	2.215	<Mn5–O>	2.215	As3–O11	1.679(11)
				As3–O12	1.701(10)
Mn3–O1	2.101(11)	Mn6–O7	2.059(12)	<As3–O>	1.671
Mn3–O10	2.147(12)	Mn6–O2	2.107(11)		
Mn3–O15	2.163(11)	Mn6–O12	2.121(11)	As4–O13	1.656(11)
Mn3–O6	2.173(10)	Mn6–O11	2.200(11)	As4–O14	1.664(11)
Mn3–OW17	2.253(11)	Mn6–OW23	2.230(13)	As4–O15	1.679(10)
Mn3–OW18	2.340(11)	<Mn6–O>	2.143	As4–O16	1.695(10)
<Mn3–O>	2.196			<As4–O>	1.674
Hydrogen bonds					
OW17–O5	2.619(16)	OW20–O1	2.651(15)	OW23–O2	2.704(17)
OW17–O14	2.664(15)	OW20–O15	3.009(15)	OW23–O13	2.749(16)
OW18–OW24	2.667(18)	OW21–O2	2.617(18)	OW24–OW23	2.69(2)
OW18–O9	2.864(14)	OW21–O9	2.878(18)	OW24–O14	3.018(19)
OW19–O14	2.655(15)	OW22–OW24	2.85(2)		
OW19–O5	2.716(15)	OW22–OW20	3.06(2)		

Table 6. Bond-valence analysis for castellaroite. Values are expressed in valence units.

	Mn1	Mn2	Mn3	Mn4	Mn5	Mn6	As1	As2	As3	As4	hydrogen bonds	Σ_a
O1			0.43				1.39				+0.25	2.07
O2						0.42	1.31				+0.28, + 0.22	2.23
O3	0.42	0.36					1.27					2.05
O4				0.32	0.29		1.23					1.84
O5								1.35			+0.27, + 0.22	1.84
O6	0.33		0.36					1.29				1.98
O7					0.28	0.48		1.25				2.01
O8		0.39		0.37				1.23				1.99
O9	0.41								1.43		+0.16, + 0.16	2.16
O10			0.38	0.35					1.30			2.03
O11					0.30	0.33			1.27			1.90
O12		0.30				0.41			1.20			1.91
O13					0.43					1.35	+0.20	1.98
O14										1.32	+0.25, + 0.25, + 0.13	1.95
O15	0.43		0.36							1.27	+0.13	2.19
O16		0.40		0.42						1.21		2.03
OW17		0.28	0.29								–0.25,–0.27	0.05
OW18			0.23	0.22							–0.16,–0.24	0.05
OW19	0.30			0.30							–0.22,–0.25	0.13
OW20	0.14	0.22									+0.12,–0.13,–0.25	0.10
OW21					0.37						–0.16,–0.28	–0.07
OW22					0.26						–0.12,–0.17	–0.03
OW23						0.30					+0.23,–0.20,–0.22	0.11
OW24											+0.17, + 0.24,–0.13,–0.23	0.05
Σ_c	2.16	1.97	2.02	1.96	1.94	1.90	5.13	4.94	5.32	5.01		

Bond valence parameters from Brown & Altermatt (1985). Hydrogen-bond strengths based on O–O bond distances from Ferraris & Ivaldi (1988). Half-occupied OW25 and OW26 sites are not included. Donated and accepted hydrogen bonds are indicated by – and +, respectively.

7. Discussion of the structure

In the structure of castellaroite, there are four different AsO_4 tetrahedra, five different MnO_6 octahedra and one MnO_5 square pyramid. The octahedra centred by Mn1, Mn2, Mn3 and Mn4 share edges forming kinked chains parallel to [100]. The chains are linked to each other by corner-sharing, forming sheets parallel to {001}. All four AsO_4 tetrahedra corner-link with octahedra in the sheet, forming a heteropolyhedral layer (Fig. 4). The $Mn5O_6$–$Mn6O_5$ edge-sharing dimers are located between the heteropolyhedral layers and share corners with octahedra and tetrahedra in adjacent layers, thereby linking the layers in the [001] direction.

The heteropolyhedral layer is topologically identical to those in the structures of several phosphate minerals: angarfite, $NaFe^{3+}{}_5(PO_4)_4(OH)_4{\cdot}4H_2O$ (Kampf *et al*., 2012), bakhchisaraitsevite, $Na_2Mg_5(PO_4)_4{\cdot}7H_2O$ (Liferovich *et al*., 2000; Yakubovich *et al*., 2000), mejillonesite, $NaMg_2(PO_3OH)(PO_4)(OH){\cdot}(H_3O + H_2O)$ (Atencio *et al*., 2012), metaswitzerite, $Mn_3(PO_4)_2{\cdot}4H_2O$ (formerly switzerite; Fanfani & Zanazzi, 1979), rimkorolgite, $BaMg_5(PO_4)_4{\cdot}8H_2O$ (Krivovichev *et al*., 2002) and switzerite, $Mn_3(PO_4)_2{\cdot}7H_2O$ (Zanazzi *et al*., 1986). Castellaroite is the first arsenate with this type of heteropolyhedral layer. The interlayer region in the structure of castellaroite is different from that in any of these structures, but it is most similar to that in metaswitzerite, which except for the configuration of $Mn5O_6$ and $Mn6O_5$ polyhedra, could be regarded as the PO_4 analogue of castellaroite.

In the metaswitzerite structure, pairs of $Mn6O_5$ pyramids form edge-sharing dimers and $Mn5O_6$ octahedra do not share edges with any other polyhedra. Although the linkages in both structures result in heteropolyhedral frameworks, the castellaroite framework contains continuous channels along [100], while the metaswitzerite framework contains discontinuous cavities. Isolated H_2O groups are contained in the channels in castellaroite (O24, O25 and O26) and the cavities in metaswitzerite (O24). The structures of castellaroite and metaswitzerite are compared in Fig. 5.

The layers in the structure of switzerite, including outlying MnO_6 octahedra, are linked to adjacent layers only by hydrogen bonds through isolated H_2O groups in the interlayer region. Switzerite transforms readily to metaswitzerite by losing ¾ of its isolated H_2O groups resulting in the condensation of the layers into the framework noted above (Zanazzi *et al*., 1986). An arsenate equivalent of switzerite, which could correspond to a hydrated precursor to castellaroite, is not known. Manganohörnesite, $Mn_3(AsO_4)_2{\cdot}8H_2O$, a member of the vivianite group, has a structure very different from that of switzerite and cannot transition to castellaroite through dehydration via simple structural condensation.

It is worth noting that sterlinghillite, $Mn_3(AsO_4)_2{\cdot}3H_2O$ (Dunn, 1981; Matsubara *et al*., 2000), which has been found with castellaroite, has 1½ less H_2O groups *pfu*. Its structure has never been determined; however, its powder XRD pattern is quite distinct from that of castellaroite. The sterlinghillite from the Monte Nero mine that we examined occurs as subparallel intergrowths of tiny plates. The plates are distinctly brittle and much harder than castellaroite. Unfortunately, efforts to separate a plate suitable for single-crystal study were unsuccessful.

Acknowledgements: The paper benefited from comments by an anonymous reviewer. This study was funded by the John Jago Trelawney Endowment to the Mineral Sciences Department of the Natural History Museum of Los Angeles County.

References

Atencio, D., Chukanov, N.V., Nestola, F., Witzke, T., Coutinho, J. M.V., Zadov, A.E., Contreira Filho, R.R., Färber, G. (2012): Mejillonesite, a new acid sodium, magnesium hydrogen phosphate mineral from Mejillones, Antofagasta, Chile. *Am. Mineral*., **96**, 19–25.

Brown, I.D. & Altermatt, D. (1985): Bond-valence parameters from a systematic analysis of the inorganic crystal structure database. *Acta Crystallogr*., **B41**, 244–247.

Burla, M.C., Caliandro, R., Camalli, M., Carrozzini, B., Cascarano, G.L., Giacovazzo, C., Mallamo, M., Mazzone, A., Polidori, G., Spagna, R. (2012): *SIR2011*: a new package for crystal structure determination and refinement. *J. Appl. Crystallogr*., **45**, 357–361.

Callegari, A.M., Boiocchi, M., Ciriotti, M., Balestra, C. (2012): Coralloite, $Mn^{2+}Mn^{3+}{}_2(AsO_4)_2(OH)_2{\cdot}4H_2O$, a new mixed valence Mn hydrate arsenate: Crystal structure and relationships with bermanite and whitmoreite mineral groups. *Am. Mineral*., **97**, 727–734.

Cámara, F., Ciriotti, M.E., Bittarello, E., Nestola, F., Massimi, F., Radica, F., Costa, E., Benna, P., Piccoli, G.C. (2014): Arsenic-bearing new mineral species from Valletta mine, Maira Valley, Piedmont, Italy: I. Grandaite, $Sr_2Al(AsO_4)_2(OH)$, description and crystal structure. *Mineral. Mag*., **78**, 757–774.

Cámara, F., Bittarello, E., Ciriotti, M.E., Nestola, F., Radica, F., Marchesini, M. (2015): As-bearing new mineral species from Valletta mine, Maira Valley, Piedmont, Italy: II. Braccoite, $NaMn^{2+}{}_5[Si_5AsO_{17}(OH)](OH)$, description and crystal structure. *Mineral. Mag*., **79**, 171–189.

Cámara, F., Bittarello, E., Ciriotti, M.E., Nestola, F., Radica, F., Massimi, F., Balestra, C., Bracco, R. (2016): As-bearing new mineral species from Valletta mine, Maira Valley, Piedmont, Italy: III. Canosioite, $Ba_2Fe^{3+}(AsO_4)_2(OH)$, description and crystal structure. *Mineral. Mag*., DOI: 10.1180/minmag.2016.080.097

Dunn, P.J. (1981): Sterlinghillite, a new hydrated manganese arsenate mineral from Ogdensburg, New Jersey. *Am. Mineral*., **66**, 182–184.

Fanfani, L. & Zanazzi, P.F. (1979): Switzerite: its chemical formula and crystal structure. *Tschermaks Min. Petr. Mitt*., **26**, 255–269.

Ferraris, G. & Ivaldi, G. (1988): Bond valence vs. bond length in O…O hydrogen bonds. *Acta Crystallogr*., B44, 341–344.

Higashi, T. (2001): *ABSCOR*. Rigaku Corporation, Tokyo.

Kampf, A.R., Mills, S.J., Housley, R.M., Boulliard, J.-C., Bourgoin, V. (2012): Angarfite, $NaFe^{3+}R_5(PO_4)_4(OH)_4{\cdot}4H_2O$, a new mineral from the Angarf-Sud pegmatite, Morocco: description and crystal structure. *Can. Mineral*., **50**, 781–791.

Krivovichev, S.V., Britvin, S.N., Burns, P.C., Yakovenchuk, V.N. (2002): Crystal structure of rimkorolgite, $Ba[Mg_5(H_2O)_7(PO_4)_4](H_2O)$, and its comparison with bakhchisaraitsevite. *Eur. J. Mineral*., **14**, 397–402.

Liferovich, R.P., Pakhomovsky, Ya.A., Yakubovich, O.V., Massa, W., Laajoki, K., Gehör, S., Bogdanova, A.N., Sorokhtina, N.V. (2000): Bakhchisaraitsevite, $Na_2Mg_5[PO_4]_4{\cdot}7H_2O$, a new mineral from hydrothermal assemblages related to phoscorite–carbonatite complex of the Kovdor massif, Russia. *Neues Jb. Miner. Mh.*, 2000, 402–418.

Mandarino, J.A. (2007): The Gladstone–Dale compatibility of minerals and its use in selecting mineral species for further study. *Can. Mineral*., **45**, 1307–1324.

Marchesini, M. & Pagano, R. (2001): The Val Graveglia manganese district, Liguria, Italy. *Mineral. Rec*., **32**, 349–379. 415.

Marescotti, P. & Cabella, R. (1996): Significance of chemical variations in a chert sequence of the "Diaspri di Monte Alpe" formation (Val Graveglia, northern Apennine, Italy). *Ofioliti*, **21**(2), 139–144.

Martens, W.N., Kloprogge, J.T., Frost, R.L., Rintoul, L. (2004): Single-crystal Raman study of erythrite, $Co_3(AsO_4)_2{\cdot}8H_2O$. *J. Raman Spectrosc*., **35**(3), 208–216.

Matsubara, S., Miyawaki, R., Mouri, T., Kitamine, M. (2000): Sterlinghillite, a rare manganese arsenate, from the Gozaisho mine, Fukushima Prefecture, Japan. *Bull. Natl. Sci. Mus. Series C*, **26**(1–2), 1–7.

Pouchou, J.-L. & Pichoir, F. (1991): Quantitative analysis of homogeneous or stratified microvolumes applying the model "PAP". in "Electron probe quantitation", K.F.J. Heinrich and D.E. Newbury, eds. Plenum Press, New York, 3l–75.

Sheldrick, G.M. (2008): A short history of *SHELX*. *Acta Crystallogr*., **A64**, 112–122.

Wilson, A.J.C. (editor) (1992): International Tables for Crystallography. Volume C: Mathematical, physical and chemical tables. Kluwer Academic Publishers, Dordrecht, The Netherlands.

Wojdyr, M. (2010): Fityk: a general-purpose peak fitting program. *J. Appl. Crystallogr*., **43**, 1126–1128.

Yakubovich, O.V., Massa, W., Liferovich, R.P., Pakhomovsky, Y.A. (2000): The crystal structure of bakhchisaraitsevite, $[Na_2(H_2O)_2]\{(Mg_{4.5}Fe_{0.5})(PO_4)_4(H_2O)_5\}$, a new mineral species of hydrothermal origin from the Kovdor phoscorite-carbonatite complex, Russia. *Can. Mineral*., **38**, 831–838.

Zanazzi, P.F., Leavens, P.B., White, J.S. (1986): Crystal structure of switzerite, $Mn_3(PO_4)_2{\cdot}7H_2O$, and its relationship to metaswitzerite, $Mn_3(PO_4)_2{\cdot}4H_2O$. *Am. Mineral*., **71**, 1224–1228.

Received 6 January 2016
Modified version received 22 February 2016
Accepted 24 February 2016